



In Silico Docking, Enzyme Inhibition Assay of the Bioactive Compounds Isolated from *Fusarium oxysporum*

Faheem Ullah¹, Bashir Ahmad^{1*}, Shumaila Rauf², Abid Ali Khan^{1*}

¹Centre of Biotechnology and Microbiology, University of Peshawar, Pakistan

²Department of Pharmacy, University of Peshawar, Pakistan

Key words: 8-O-methylbostrycoidin, 9-O-methylanhydrofusarubin, *Fusarium oxysporum*, Carbonic anhydrase.

<http://dx.doi.org/10.12692/ijb/16.2.421-435>

Article published on February 24, 2020

Abstract

Two naphthoquinones; 8-O-methylbostrycoidin (**1**) and 9-O-methylanhydrofusarubin (**2**) were purified from the ethyl acetate fraction of the crude from *Fusarium oxysporum* and characterized through spectrometric techniques. These metabolites were tested against phosphodiesterase-I, urease and carbonic anhydrase-II. Both the naphthoquinones displayed substantial inhibition of phosphodiesterase-1 with IC₅₀ value of 65 ± 3.01 and 30.10 ± 2.12 µM, respectively when compared with the standard EDTA (IC₅₀ = 24 ± 0.22). Similarly, both the compounds showed significant activity against urease with IC₅₀ values equal to 45 ± 1.45 and 67 ± 6.23 µM, respectively, while thiourea was used as standard for urease inhibition assay with IC₅₀ value of 21 ± 0.12 µM. Most significant activity was observed against carbonic anhydrase-II for both of the compounds (86.31% and 73.80% inhibition, respectively) as compared to the standard acetazolamide (89.44%). Absorption, distribution, metabolism and excretion (ADME) properties of both compounds were calculated using SwissADME server, and showed considerable scores of drug properties. Molecular docking studies were performed for both the compounds using PatchDock server. It was observed that the binding affinities of compound (**1**) are -101.64, -117.32 and -93.19 kcal/mol (atomic contact energy (ACE) of Patchdock) with PDE, urease and carbonic anhydrase, respectively and stands comparatively better than the standards; i.e., -80.77 (EDTA), -69.61 (thiourea) and -49.25 kcal/mol (Acetazolamide). Similarly, the binding affinities of compound (**2**) are higher with the receptor proteins (-87.76, -86.20 and -92.12 kcal/mol with PDE, urease and carbonic anhydrase, respectively) than the standard inhibitors (-80.77 (EDTA), -69.61 (thiourea) and -49.25 kcal/mol (Acetazolamide)).

* Corresponding Author: Bashir Ahmad ✉ bashirdr2015@yahoo.com

Introduction

Fungi produce a vast array of organic compounds, which are not required for their metabolic activities and are called secondary metabolites. In recent decades, bioactive natural products obtained from the medicinal plant endophytic fungi have attracted the rising attention due to their diverse pharmacological activities, such as anti-inflammatory (Pretsch *et al.*, 2014; Weber *et al.*, 2004), antimicrobial (Khan *et al.*, 2013; Luo *et al.*, 2007), antioxidant (Strobel *et al.*, 2002) and antitumor activities (Deng *et al.*, 2013). Researchers have modified the conditions for the augmented production of these bioactive compounds by fungi (Khan *et al.*, 2017).

Phosphodiesterase (PDE) (EC 3.1.4.1) is a group of biological catalysts (enzymes) which are responsible for the breakdown of cyclic adenosine monophosphate (cAMP) and cyclic guanosine Monophosphate (cGMP). They (cAMP & cGMP) play crucial role in regulation of human heart muscles (myocardium) by inotropic mechanisms. There are some therapeutic drugs which inhibit the activity of PDE by hindering or slowing down the production of cAMP and thus hampering the effect of PDE on heart, lungs, platelet function and other inflammatory effects of PDE. Urease (EC 3.5.1.5) is a hydrolyzing enzyme which belongs to the amidohydrolases superfamily. It is capable of converting urea into ammonia and carbonic acid. It is widely present in both prokaryotes (bacteria) and eukaryotes (fungi and plants)(Li *et al.*, 2014). The products of urease, i.e. ammonia and carbonic acid are toxic to human tissues (Dunn & Phadnis, 1998; Follmer, 2010) and can result in life-long human disorders like rheumatoid arthritis and atherosclerosis (Arabski *et al.*, 2010; Konieczna *et al.*, 2012). Carbonic anhydrases are group of enzymes, which catalyzes the hydration of carbon dioxide to bicarbonate and hydrogen ion (proton). Inhibitors of carbonic anhydrase may be bicarbonatoretic, kaluretic or natriuretic if they increase the excretion of bicarbonates, potassium or sodium ions, respectively in urine (Vardanyan & Hrubby, 2016). The hunt for novel enzyme inhibitors can be helpful in controlling

and curing numerous diseases related to enzyme activity. Thus, there is a strong need of searching new compounds with potential anti-enzymatic activity which can be used as therapeutics in future. In this study, the enzyme inhibition assay was confirmed using molecular docking analysis.

Materials and methods

Isolation and purification of Fusarium oxysporum

Fusarium oxysporum was isolated from the root culture of *Narium indicum* and was purified on PDA medium. The fungus was identified by its microscopic examination using slide culture method.

Extraction of fungal secondary metabolites and their characterization

The fungus was grown in saboraud dextrose broth (SDB) medium and incubated at 29-30°C for 18 days at pH 5. After incubation period, the concentrated HCl was added to settle the culture medium. The culture medium was blended and filtered through cheese cloth to separate the fungal mycelia and spores. To the filtrate, equal volume of ethyl acetate was added, shook and then transferred to the separating funnel. The ethyl acetate fraction was isolated and washed with brine solution (2M). After washing with brine solution, the ethyl acetate fraction was purified with anhydrous sodium sulphate (Na₂SO₄) and was concentrated in the rotary evaporator at 60 °C at 150 rpm.

The ethyl acetate fraction was then subjected to column chromatography and TLC and two compounds (1 & 2) were purified. The structures of the compounds were elucidated from the analysis of their spectra data.

Prediction of Cheminformatics and Bioactivity Properties of Ligand Molecules

Molinspiration(Cheminformatics, 2015) web-based server was used to predict biological properties of ligand molecules such as GPCR ligand, ion channel modulator, kinase inhibition, protease inhibition, etc. To predict the Adsorption, Distribution, Metabolism and Excretion (ADME) properties, drug likeness and

pharmacokinetics properties of the ligand molecules, another web-based server SwissADME(Daina *et al.*, 2017)was used.

Enzyme inhibition assay

Urease Inhibition Assay: Kakiuchi(Kakiuchi *et al.*, 1975)method with few changes was followed for the urease inhibition assay. Five microliters of the test compound were incubated with 25 μ L of 0.25 mg/ml of enzyme for 15 minutes at 37°C. Then, the same mixture with 55 μ L of urea as substrate was incubated for another 15 minutes at 37°C. Absorbance of the mixture was determined at 630 nm after the incubation period and readings were noted. After that, alkali solution (70 μ L) and phenol (45 μ L) was added to the mixture and incubated at 37°C for 50 minutes. After incubation period, absorbance was measured at 630 nm. Methanol and thiourea were used at negative and positive controls, respectively.

Carbonic Anhydrase Assay: Şentürk(Şentürk *et al.*, 2011) method was followed for the carbonic anhydrase assay.

Phosphodiesterase-1 Assay: Perry and Higgs(Perry & Higgs, 1998) procedure, with few alterations, was used for the phosphodiesterase-1 inhibition assay. The enzyme (0.000742 U) were taken and 30 mM magnesium acetate and 33 mM tris-HCl with pH 8.8 were mixed as co-factors in flat-bottom 96-well microtiter plate. The substrate used was bis-*p*-nitrophenyl phosphate (0.33 mM). The reference compound used in the assay was ethylene diamine tetra acetic acid (EDTA). The microtiter plate was incubated for 30 minutes at 37°C. After incubation period, absorbance was measured at 410 nm using microtiter plate reader spectrophotometer.

Molecular Docking

The 3D crystallographic structures of the target proteins (Phosphodiesterase-1 (ID: 5GZ4), urease (ID: 4GY7) and carbonic anhydrase (ID: 1BN1)) were retrieved from Protein Data Bank (PDB). The 3D structures of the target proteins were refined using ModRefiner(Xu & Zhang, 2011). The errors in the theoretical and experimental structures were recognized using ProSA (Protein Structure Analysis)(Sippl, 1993; Wiederstein & Sippl, 2007) web server. VADAR(Willard *et al.*, 2003) web-based server was used to report the volume, area and dihedral angles of the refined structures.Enzyme active sites of the refined protein structures were determined using metaPocket 2.0(Zhang *et al.*, 2011).

The structure of the ligand molecules (8-O-methylbostrycoidin (**1**) & 9-O-methylanhydrofusarubin (**2**) were prepared using Chem Draw Ultra version 10.0 (Mills, 2006).

The energies of the ligands were minimized and the structures were optimized and converted to PDB format using PRODRG server(Schüttelkopf & Van Aalten, 2004).Docking studies were carried out using PatchDock (Schneidman-Duhovny *et al.*, 2005) server. The visualization of the docked complexes was carried out using BIOVIA Discovery Studio Visualizer v19.1.0.18287(BIOVIA).

Result and discussion

8-O-methylbostrycoidin (**1**)

Compound (**1**) was isolated as red crystals from the ethyl acetate fraction of *Fusarium oxysporum*. Using the HR-ESI-MS, the molecular formula of the compound was identified as C₁₆H₁₃NO₅.

Table 1. Bio-activity scores of known compounds (C-1) and (C-2) calculated by Molinspirationserver.

Bioactivities	(C-1)	(C-2)
GP.CR liga.nd	-0.06	-0.11
Ion. channel. modulator.	-0.10	-0.29
Kinase. inhibitor.	0.3.3	-0.04
Nuclear.r.eceptor. ligand.	-0.02	-0.08
Protea.se inhibit.or	-0.16	-0.32
Enzym.einhibito.r	0.28	0.21

IR (KBr, ν_{\max} in cm^{-1}): 1650, 1625, 1550, 1460, 1391, 1250. UV λ_{\max} in nm: 268, 274, 480. $^1\text{H-NMR}$ (500 MHz, CD_3Cl): δ 9.60 (1H, s, CH-1), 2.73 (3H, s, CH_3 -3), 7.95 (1H, s, CH-4), 4.14 (3H, s, CH_3O -6), 6.78 (1H, s, CH-7), 4.12 (3H, s, CH_3O -8). $^{13}\text{C-NMR}$ (500 MHz, CD_3Cl): δ 150.1 (CH, C-1), 127.8 (C, C-3), 119.5 (CH, C-4), 143.9 (C, C-5), 156.6 (C, C-6), 105.6 (CH, C-7),

157.2 (C, C-8), 186.4 (C, C-9), 189.1 (C, C-10), 120.8 (C, C-11), 110.11 (C, C-12), 127.0 (C, C-13), 147.3 (C, C-14), 124.6 (CH_3 , C-15), 55.7 (CH_3 , C-16), 57.3 (CH_3 , C-17). Based on the spectroscopic data and reported literature, the compound (**1**) was identified as 8-O-methylbostrycoidin (Fig. 1a) (Tatum *et al.*, 1985).

Table 2. Physiochemical properties, lipophilicity, water solubility, pharmacokinetics, drug likeness and medicinal chemistry properties of. Known compound (C-1).

Physiochemical Properties		Pharmacokinetics	
Formula	$\text{C}_{16}\text{H}_{13}\text{NO}_5$	*GI absorption	High
Molecular Weight	299.28 g/mol	*BBB permeant	No
No. of heavy atoms	22	*P-gp substrate	No
No. of arom. Heavy atoms	12	*CYP1A2 inhibitor	Yes
*Fraction Csp3	0.19	*CYP2C19 inhibitor	No
No. of rotatable bonds	2	*CYP2C9 inhibitor	Yes
No. of H-bond acceptors	6	*CYP2D6 inhibitor	No
No. of H-bond donors	1	*CYP3A4 inhibitor	Yes
Molar Refractivity	77.52	Log Kp (Skin permeation)	-6.46 cm/s
*TPSA	85.72 \AA^2	Druglikeness	
Lipophilicity		*Lipinski	Yes, 0 violation
Log P_o/w (iLOGP)*	2.16	*Ghose	Yes
Log P_o/w (XLOGP3)*	2.34	*Veber	Yes
Log P_o/w (WLOGP)*	1.89	*Egan	Yes
Log P_o/w (MLOGP)*	-0.20	*Muegge	Yes
Log P_o/w (SILICOS-IT)	3.05	Bioavailability Score	0.55
Consensus Log P_o/w	1.85	Medicinal Chemistry	
Water Solubility		*PAINS	1 alert quinone_A
Log S (ESOL)*	3.44	*Brenk	0 alert
Solubility	1.08e-01 mg/ml; 3.62e-04 mol/l	*Leadlikeness	Yes
Class	Soluble	Synthetic accessibility	2.67
Log S (Ali)*	3.78		
Solubility	4.97e-02 mg/ml; 1.66e-04 mol/l		
Class	Soluble		
Log S (SILICOS-IT)*	4.93		
Solubility	3.53e-03 mg/ml; 1.18e-05 mol/l		
Class	Moderately soluble		

*Fraction Csp3= Fraction of carbon in sp^3 hybridization, *TPSA= Topological Polar Surface Area, $i\text{Log } P_o/w^*$ = partition coefficient between. *n*-octanol and water, *iLOGP, XLOGP3, WLOGP, MLOGP, SILICOS-IT= Different topological methods for determining lipophilicity, *Log S (ESOL), Log. S (Ali.), Log. S (SILICOS-IT)= Different topological methods for determining water solubility, *GI= Gastrointestinal tract, *BBB= Blood-Brain-Barrier, *P-gp= Permeability Glycoprotein, *Lipinski, Ghose, Veber, Egan, Muegge= Rule-based filters to exclude fragments/molecules incompatible with acceptable pharmacokinetic profile, *PAINS= Pan Assay Interface (show compounds which gives false positive biological output) PAINS and Brenk are filters for drug-likeness, *Leadlikeness= molecular entity which is suitable to drug-likeness.

9-O-methylanhydrofusarubin (2)

Compound (2) was isolated as red crystals from the ethyl acetate fraction of *Fusarium oxysporum*. Using the HR-ESI-MS, the molecular formula of the compound was identified as C₁₆H₁₄O₆.

IR (KBr, ν_{\max} in cm⁻¹): 2970, 1670, 1625, 1450, 1391, 1230, 1150. UV λ_{\max} in nm: 213, 268, 274. ¹H-NMR (500 MHz, CD₃Cl): δ 2.81 (3H, s, CH₃-2), 4.26 (1H, s, CH-3), 4.15 (3H, s, CH₃O-6), 6.65 (1H, s, CH-7), 4.17 (3H, s, CH₃O-8). ¹³C-NMR (500 MHz, CD₃Cl): δ 156.1

(C, C-2), 90.5 (CH, C-3), 186.0 (C, C-4), 137.2 (C, C-5), 157.1 (C, C-6), 106.8 (CH, C-7), 157.2 (C, C-8), 190.0 (C, C-9), 65.5 (CH₂, C-10), 146.5 (C, C-11), 146.7 (C, C-12), 128.1 (C, C-13), 115.4 (C, C-14), 21.8 (CH₃, C-15), 58.3 (CH₃, C-16), 57.0 (CH₃, C-17).

Based on the spectroscopic data and reported literature, the compound (2) was identified as 9-O-methylanhydrofusarubin (Fig. 1b) (Tatum *et al.*, 1985).

Table 3. Physiochemical properties, lipophilicity, water solubility, pharmacokinetics, drug likeness and medicinal chemistry properties of known compound (C-2).

Physiochemical Properties		Pharmacokinetics	
Formula	C ₁₆ H ₁₄ NO ₆	G1 absorption	High
Molecular Weight	302.28 g/mol	BBB permeant	No
No. of heavy atoms	22	P-gp substrate	No
No. of arom. Heavy atoms	06	CYP1A2 inhibitor	Yes
Fraction Csp ³	0.25	CYP2C19 inhibitor	No
No. of rotatable bonds	2	CYP2C9 inhibitor	Yes
No. of H-bond acceptors	6	CYP2D6 inhibitor	No
No. of H-bond donors	1	CYP3A4 inhibitor	Yes
Molar Refractivity	76.98	Log Kp (Skin permeation)	-6.71 cm/s
TPSA	82.06 Å ²	Druglikeness	
Lipophilicity		Lipinski	Yes, 0 violation
Log _o P _{o/w} (i.LOG.P)	2.53	Ghose	Yes
Log _o P _{o/w} (X.LOG.P ₃)	2.02	Veber	Yes
Log _o P _{o/w} (WL.OGP)	2.02	Egan	Yes
Log _o P _{o/w} (ML.OGP)	-0.12	Muegge	Yes
Log _o P _{o/w} (SILICOS-IT)	2.62	Bioavailability Score	0.55
Consensus Log _o P _{o/w}	1.81	Medicinal Chemistry	
Water Solubility		PAINS	1 alert quinone_A
Log S (ESOL)	-3.06	Brenk	0 alert
Solubility	2.56e-01 mg/ml.; 8.78e-04 mol/l	Leadlikeness	Yes
Class	Soluble	Synthetic accessibility	3.64
Log _o S (Ali.)	-3.37		
Solubility.	1.29e-01 mg/ml.; 4.26e-04 mol/l		
Class	Soluble		
Log S (SILICOS-IT)	-3.63		
Solubility.	7.05e-02 mg/ml.; 2.33e-04 mol/l		
Class	Soluble		

*Fraction Csp³= Fraction of carbon in sp³ hybridization, *TPSA= Topological Polar Surface Area, *i*Log P_{o/w}*= partition coefficient between *n*-octanol and water, *iLOGP, XLOGP₃, WLOGP, MLOGP, SILICOS-IT= Different topological methods for determining lipophilicity, *Log S (ESOL), Log S (Ali.), Log S (SILICOS-IT)= Different topological methods for determining water solubility, *GI= Gastrointestinal tract, *BBB= Blood-Brain-Barrier, *P-gp= Permeability Glycoprotein, *Lipinski, Ghose, Veber, Egan, Muegge= Rule-based filters to exclude fragments/molecules incompatible with acceptable pharmacokinetic profile, *PAINS= Pan Assay Interface (show compounds which gives false positive biological output) PAINS and Brenk are filters for drug-likeness, *Leadlikeness= molecular entity which is suitable to drug-likeness.

Molinspiration cheminformatics software is a web-based server which allow the users to calculate molecular properties, molecule depiction of high quality and search for similarities. The server also

provides bio-activities of ligand molecules in the form of scores. The bio-activities includes G-protein coupled receptor ligands, nuclear receptors, ion channel modulators and kinase inhibitors. The bio-

activities of ligand molecules are shown in the form of graphs by the server. The Molinspiration results of the known compounds (C-1) and (C-2) and the graphical representation are shown in Table 1 and Fig.2.

The process of drug discovery is a multistep process takes years to discover a drug. Most of the times, after considerable efforts and consumption of time in the process of drug discovery, it comes to end with no fruitful result due to the problem in ADME (Adsorption, Distribution, Metabolism and Excretion)

and lack of understanding of the pharmacokinetic properties of the potential drug. Therefore, there is a need to predict these properties in the start of the drug discovery studies so that it can be determined whether the molecule possess such properties to be developed into a potential drug or not. SwissADME is a web-based server which provide such facility. This server calculates the physiochemical properties as well as ADME, druglike nature, friendliness to medicinal chemistry and pharmacokinetic properties of molecules. The server provides computer models as an alternative to wet lab experiments.

Table 4. Showing the observed and expected number and percentage of α -helices, β -sheets, coils and turns in the PDE, Urease and CA-II.

Proteins	Helices	β -sheets,	Coils	Turns
PDE	23%	27%	49%	22%
Urease	28%	30%	40%	24%
CA-II	11%	47%	41%	24%

Table 5. Ligands (compounds (C-1) & (C-2)) interaction with receptors Phosphodiesterase, Urease and Carbonic anhydrase-II and correspondence of reported and expected active sites.

Protein Receptor/Enzyme	PDB ID	Interacting Receptor Residues		Residues involve in Hydrogen Bonding	
		With ligand (1)	With ligand (2)	With ligand (1)	With ligand (2)
Phosphodiesterase (PDE)	5GZ4	ARG ⁴⁴⁴	ASN ⁸⁵⁰	GLN ⁸¹⁰	GLU ⁸⁰⁷
		ASP ⁴⁴⁴	ASP ⁴⁴³	GLU ⁴⁶⁷	
		ASP ⁴⁶⁵	ASP ⁴⁶⁵		
		GLN ⁸¹⁰	GLN ⁸¹⁰		
		GLU ⁴⁶⁷	GLU ⁴⁶⁴		
		GLU ⁸⁰⁷	GLU ⁸⁰⁷		
		ILE ⁸⁴⁷	ILE ⁸⁴⁹		
		ILE ⁸⁴⁹	LYS ⁴¹⁶		
		LYS ⁴¹⁶	MET ⁴⁴¹		
		MET ⁴⁴¹	PHE ⁴⁶⁸		
		PHE ⁴⁶⁸	THR ⁸¹¹		
		PHE ⁸⁴⁸	TYR ⁴¹⁸		
		SER ⁸⁵¹			
		THR ⁸¹¹			
Urease	4GY7	MET ⁷⁴⁶	MET ⁷⁴⁶	MET ⁷⁴⁶	MET ⁷⁴⁶
		VAL ⁷⁴⁴	VAL ⁷⁴⁴		
		LYS ⁷¹⁶	LYS ⁷¹⁶		
		LYS ⁷⁴⁵	LYS ⁷⁴⁵		
		LEU ⁸³⁹	LEU ⁸³⁹		
		TYR ⁴¹⁷	TYR ³²		
		TYR ⁸³⁷	TYR ⁸³⁷		
		PHE ⁸³⁸	PHE ⁷¹²		
		PHE ⁸⁴⁰	PHE ⁸³⁸		
		ARG ⁶³⁰	PHE ⁸⁴⁰		
		GLU ⁴¹⁸	SER ⁴²¹		
SER ⁴²¹	THR ³³				
Carbonic Anhydrase-II (CA-II)	1BN1	ASN ¹²⁴	ASP ⁴¹	PRO ⁸³	PRO ⁸³
		ASP ⁸⁵	ASP ⁸⁵		ASP ⁸⁵
		ASP ¹³⁹	ASP ¹³⁹		THR ²⁰⁸
		LEU ⁴⁴	ASN ¹²⁴		
		LEU ⁸⁴	LEU ⁴⁴		
		LYS ²⁵⁷	LEU ⁸⁴		
		PRO ¹⁹⁵	LYS ²⁵⁷		
		THR ²⁰⁸	PRO ⁸³		
		TYR ⁸⁸	PRO ¹³⁸		
			PRO ¹⁹⁵		
	THR ²⁰⁸				
	TYR ⁸⁸				

Bioavailability radar shows six properties (lipophilicity, size, polarity, insolubility, in-saturation and flexibility) of druglikeness. The pink area (Fig.3) fall entirely in drug-like nature. The swissADME provide information about physiochemical properties,

lipophilicity, water solubility, pharmacokinetics, drug likeness and medicinal chemistry(Daina *et al.*, 2017).SwissADME properties of compounds (C-19) and (C-20) are given in Table 2 and 3, respectively.

Table 6. Receptor-ligand interaction outline of compounds. (C-1) and (C-2) and standard inhibitor with PDE, Urease and CA-II.

S.No	Receptor-ligand	No. of H-bonds	Bond Length	ACE
1.	PDE - (C-1)	2 Bonds	2.67Å GLU ⁴⁶⁷ 3.22Å GLN ⁸¹⁰	-101.64 kcal/mol
2.	PDE - (C-2)	1 Bond	1.85Å GLU ⁸⁰⁷	-87.76 kcal/mol
3.	PDE - EDTA	1 Bond	2.50Å ARG ⁷¹⁶	-80.77 kcal/mol
4.	Urease - (C-1)	1 Bond	2.15Å MET ⁷⁴⁶	-117.32 kcal/mol
5.	Urease - (C-2)	1 Bond	1.87Å MET ⁷⁴⁶	-86.20 kcal/mol
6.	Urease - Thiourea	3 Bonds	2.01 Å THR ⁵⁷⁸ 2.46 Å THR ⁵⁸⁷ 2.96 Å PRO ⁵⁷³	-69.61 kcal/mol
7.	CA-II - (C-1)	1 Bond	2.17Å PRO ⁸³	-93.19 kcal/mol
8.	CA-II - (C-2)	3 Bonds	2.27Å ASP ⁸⁵ 1.52Å PRO ⁸³ 3.23Å THR ²⁰⁸	-92.12 kcal/mol
9.	CA-II - Acetazolamide	1 Bond	2.89Å TYR ⁷	-49.25 kcal/mol

The BOILED-Egg is another graphical representation of two intuition parameters. The first one is the passive absorption by the gastrointestinal tract and the other one shows access to the brain (BBB-blood-brain-barrier passive absorption). The graph is in the form of boiled egg. The yellow yolk shows access to

the brain while the white portion shows passive absorption by the gastrointestinal tract. The molecule is colored in red (non-substrate of Permeability glycoprotein (P-gp)) or blue (substrate of P-gp). Our compounds are colored red which means that they are non-substrate of P-gp (Fig.4a &4b).

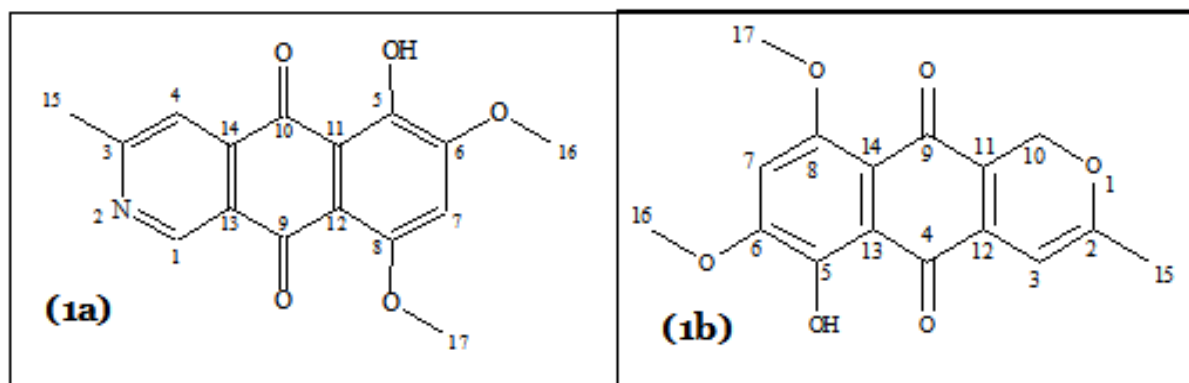


Fig. 1. Structures of compounds isolated from *Fusarium oxysporum* (1a: 8-O-methylbostrycoidin, 1b: 9-O-methylanthydrofusarubin).

For the identification of errors in the protein structure, ProSA web server was used. This server identifies and recognize errors in the protein structure. The server provides the information of the input structure in the form of a z-score plot. The plot shows a range of colors (Fig.5) which indicates the native structures from X-ray and NMR sources. If the z-score of an input structure is not in this range, it

contains errors. All the three proteins were in the range on native protein structure. The VADAR server contains 15 algorithms and programs to determine the number of α -helices, β -sheets, coils and turns in the polypeptide chain of a protein using the NMR and X-ray crystallographic data of the protein. The VADAR data of PDE, Urease and CA-II is shown in the Table 4.

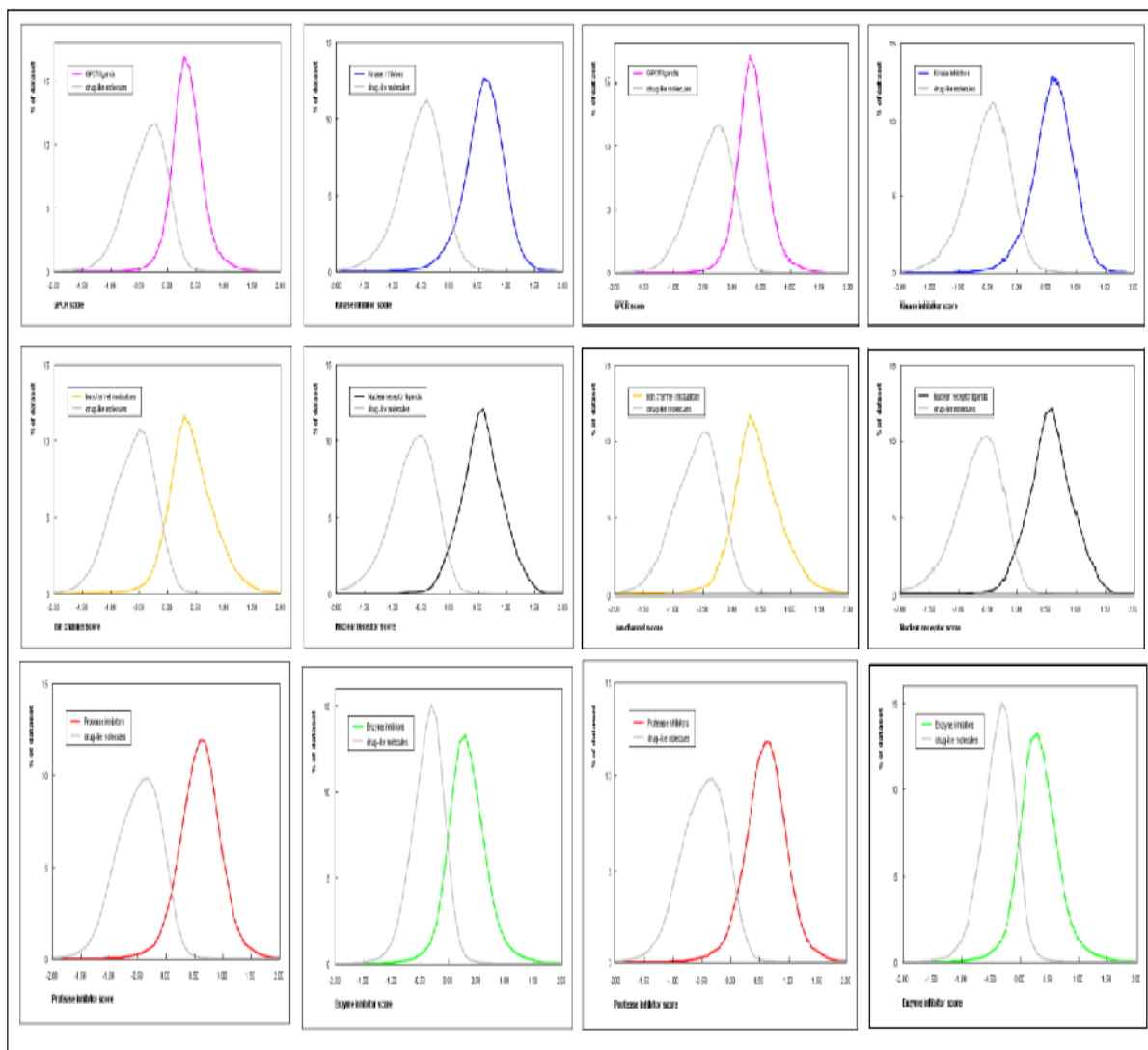


Fig. 2. Graphical representation of bio-activity predicted by Molinspiration of known compound C-1 (left) C-2 (right) and plotted against standard drugs.

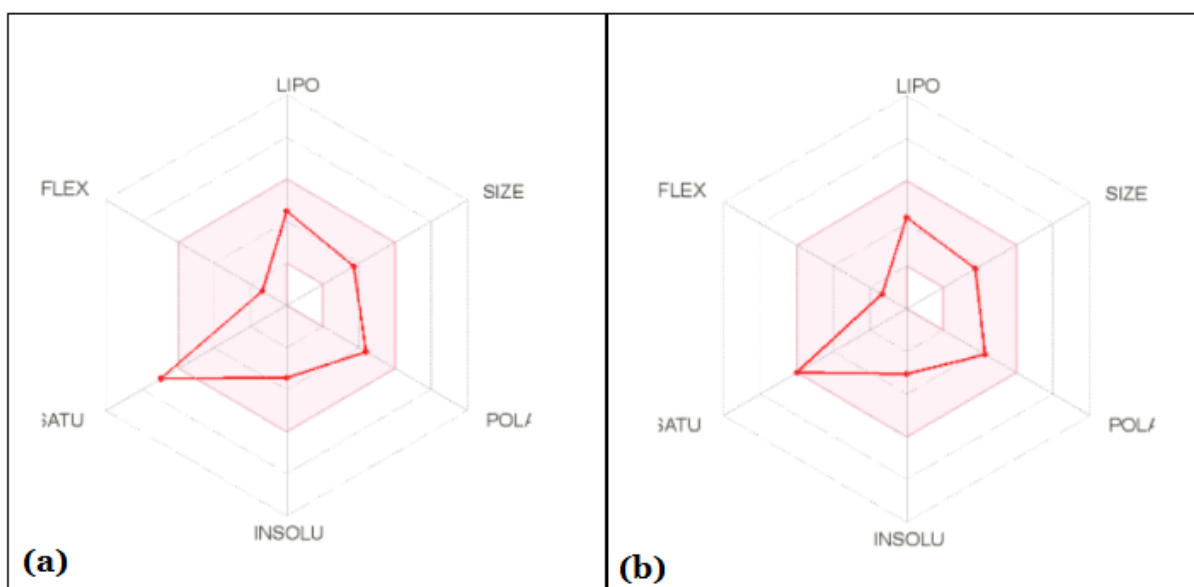


Fig. 3. Bioavailability radar of compounds (C-1) and (C-2).

The binding residues of the three receptors (PDE, Urease and CA-II) active sites and the residues involved in the hydrogen bonding (H-bonding) are shown in Table 5. Molecular docking was performed

using PatchDock server. The server was optimized to resolve 1000 receptor-ligand interactions and to select the top 10 interactions.

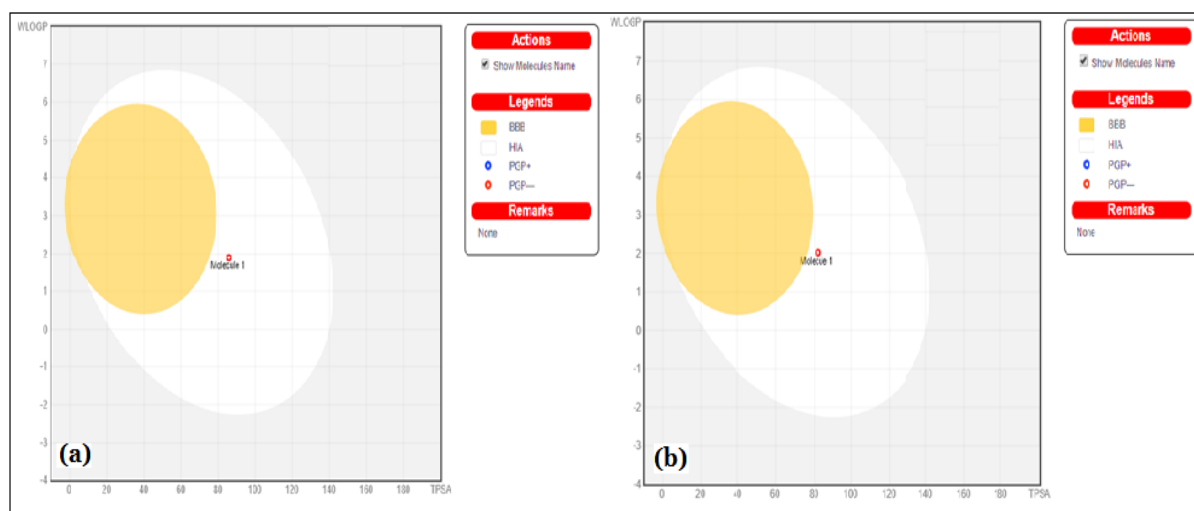


Fig. 4. The BOILED Egg representation of (a) compound (C-1) and (b) (C-2). The yellow area shows the access of the compound to the brain while the white area shows the passive absorption by the gastrointestinal tract. The molecules are represented by red circles which means that they are non-substrates of permeability glycoprotein.

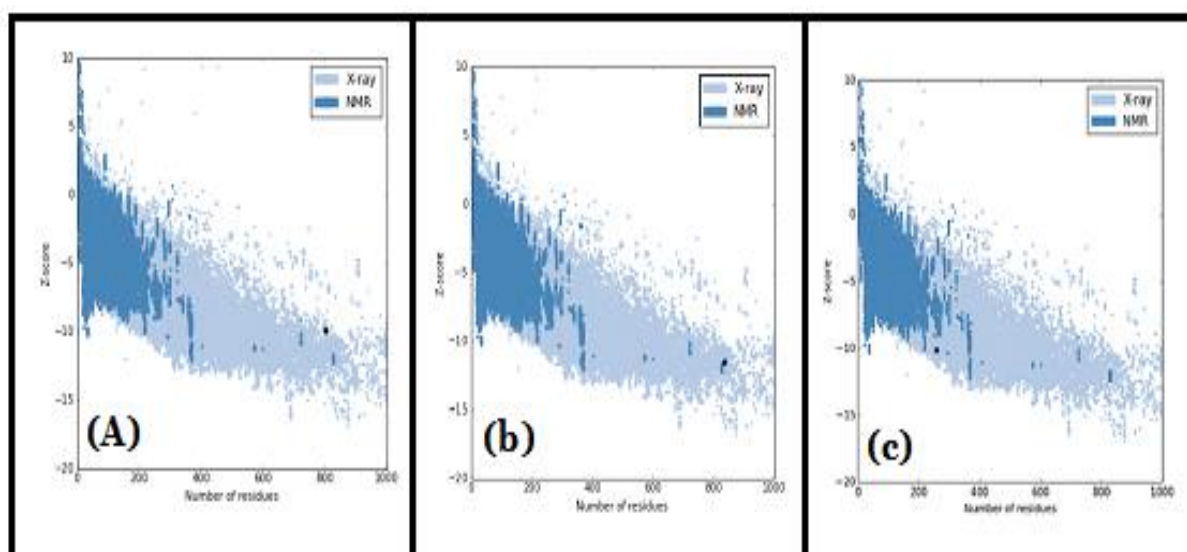


Fig. 5. The Z-score plot of (a) the refined PDE and (b) Urease (c) Carbonic anhydrase proteins structure. The black dot shows that all protein structures are within the range of Z-score.

The top 10 interactions of receptor-ligand were downloaded and analyzed by using BIOVIA Discovery Studio Visualizer v19. The binding energy, bond length and best position of the ligand in the binding site of receptor was also resolved by BIOVIA Discovery Studio Visualizer v19. The binding interactions of the receptors and ligands are shown in

Figures 6-10. The profile of receptor-ligand interaction is given in the Table 6.

It is depicted from the analysis of the receptor-ligand interactions that the ligand (C-1) form two stable H-bonds with PDE residues Glu467 and Gln810 with bond length 2.67Å and 3.22Å, respectively.

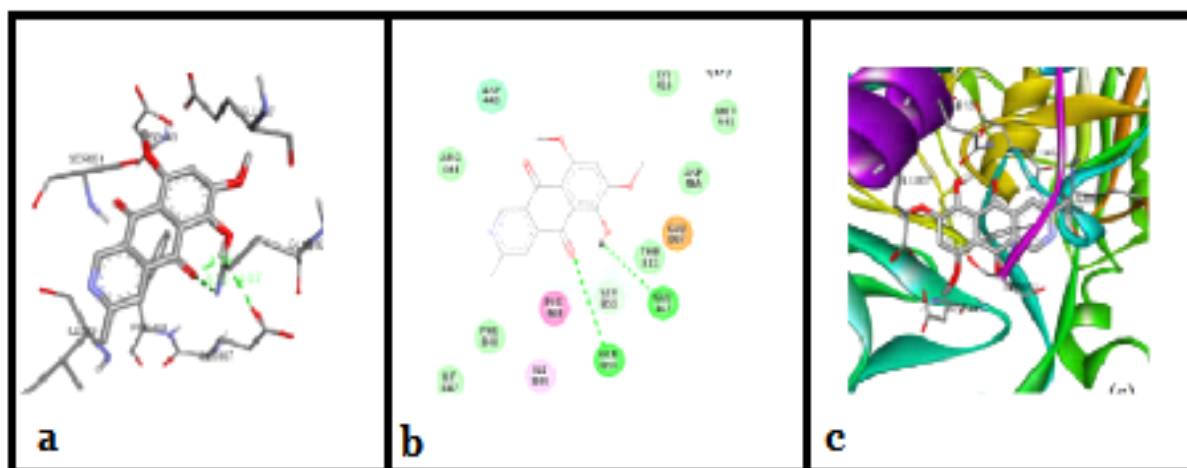


Fig. 6. Figure showing the 3D (a) and 2D (b) ligand interaction of (C-1) with interacting receptor (PDE) residues and the position of ligand in the binding site of receptor (c).

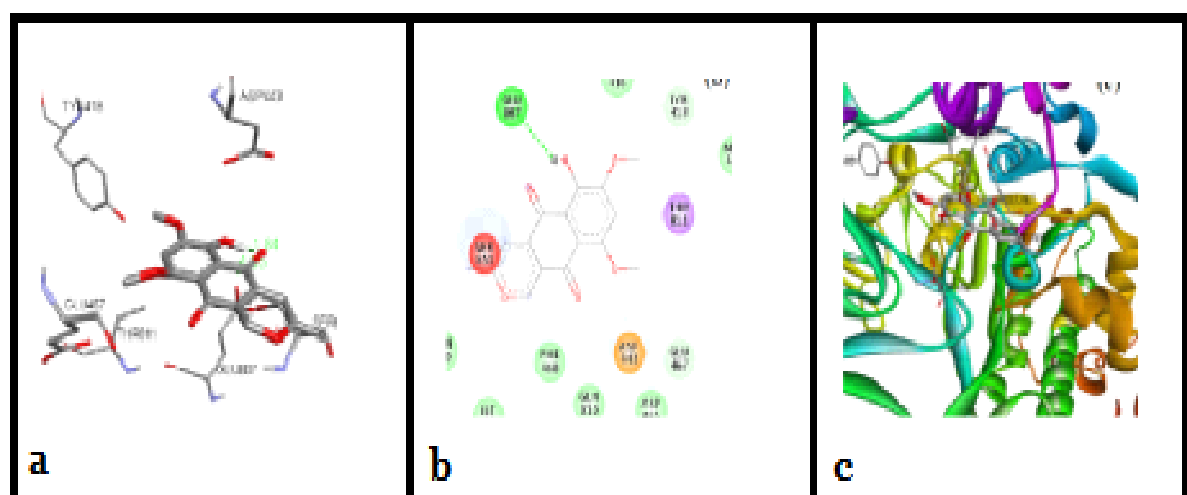


Fig. 7. Figure showing the 3D (a) and 2D (b) ligand interaction of (C-2) with interacting receptor (PDE) residues and the position of ligand in the binding site of receptor (c).

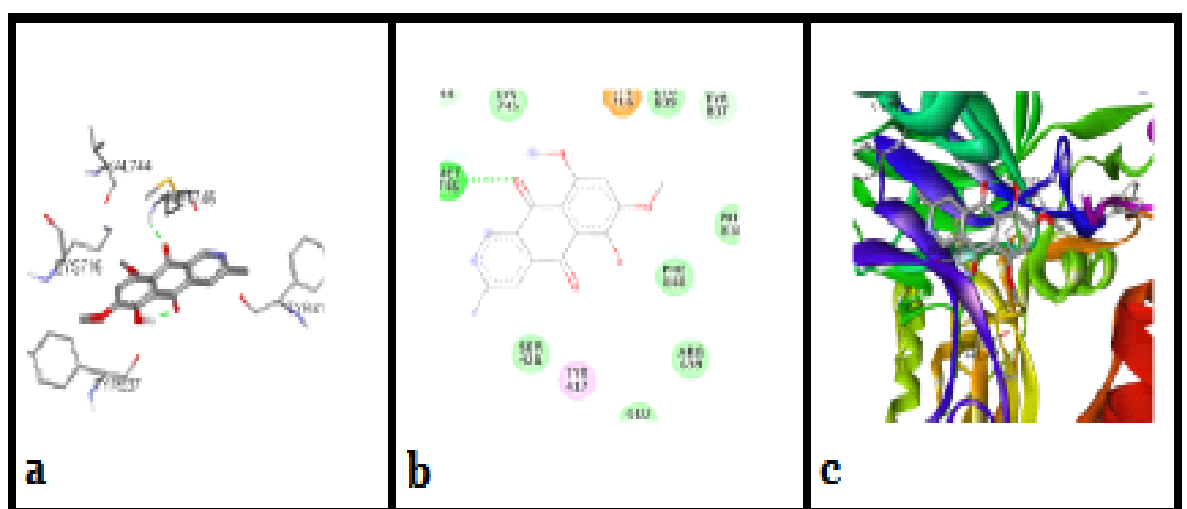


Fig. 8. Figure showing the 3D (a) and 2D (b) ligand interaction of (C-1) with interacting receptor (Jack bean urease) residues and the position of ligand in the binding site of receptor (c).

The atomic contact energy (ACE) was observed - 101.64 kcal/mol. The atoms of the ligand involve in the bonding are nitrogen and oxygen (Fig.6 (a, b, c)).

The ligand (C-20) form on H-bond with the Glu807 of PDE with bond length equal to 1.85Å (Fig. 7(a, b, c)) and bond energy equal to -87.76 kcal/mol.

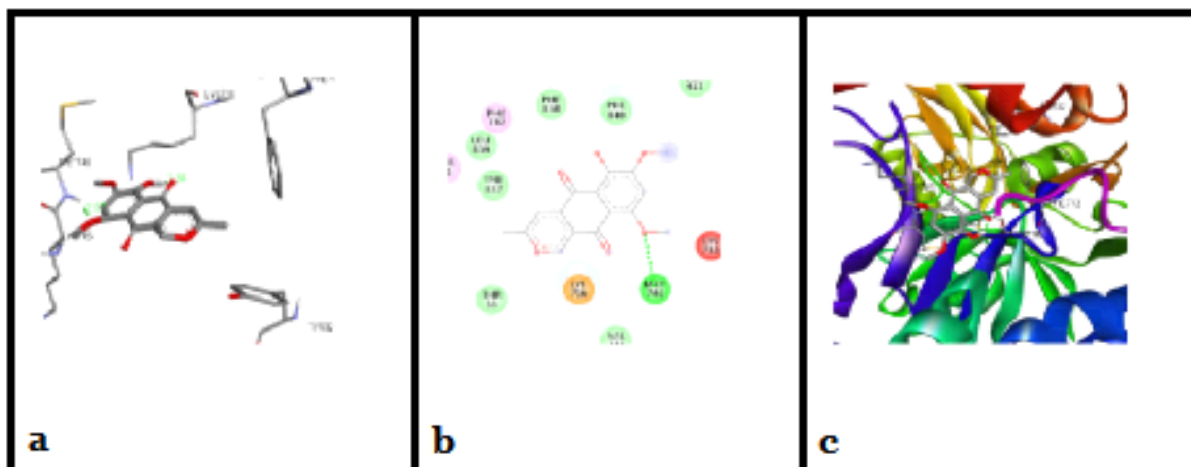


Fig. 9. Figure showing the 3D (a) and 2D (b) ligand interaction of (C-2) with interacting receptor (Jackbean urease) residues and the position of ligand in the binding site of receptor (c).

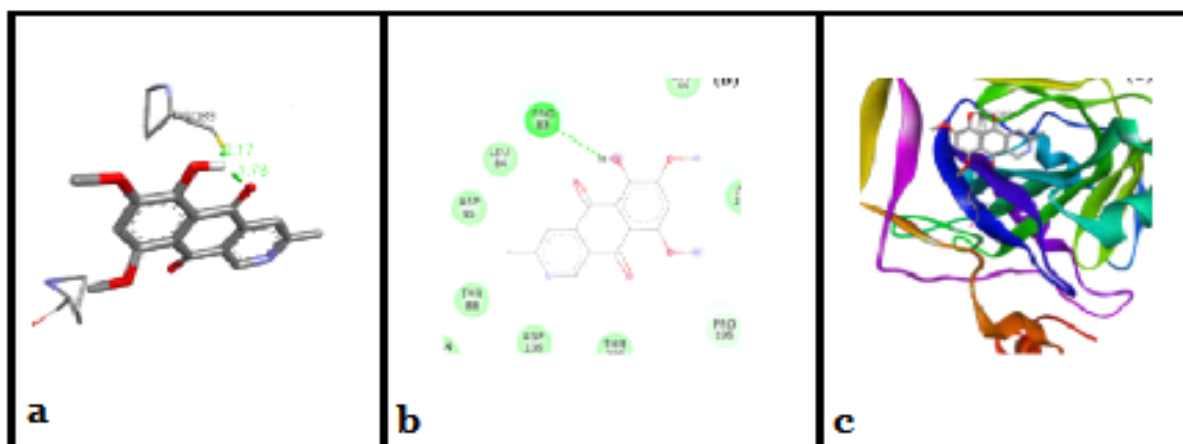


Fig. 10. Figure showing the 3D (a) and 2D (b) ligand interaction of (C-1) with interacting receptor (CA-II) residues and the position of ligand in the binding site of receptor (c).

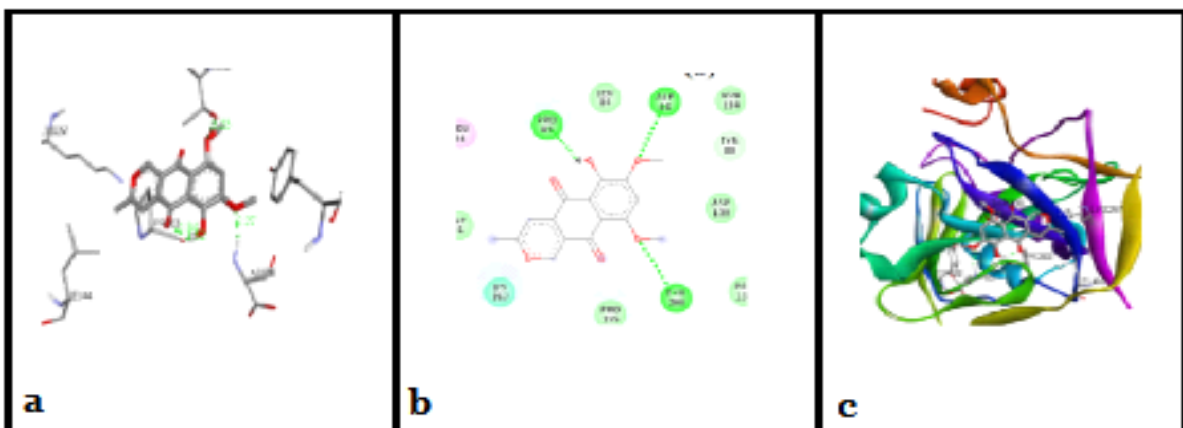


Fig. 11. Figure showing the 3D (a) and 2D (b) ligand interaction of (C-2) with interacting receptor (CA-II) residues and the position of ligand in the binding site of receptor (c).

The oxygen atom of the ligand (C-1) form a stable H-bonds with Met746 of jack bean urease with bond length 2.15Å (Fig.8 (a, b, c)). The ACE was found equal to -117.32 kcal/mol. The Met746 in the active

site of the jack bean urease forms a hydrogen with the oxygen atom of the ligand (C-2) with bond length 1.87Å and ACE -86.20 kcal/mol (Fig.9 (a, b, c)).

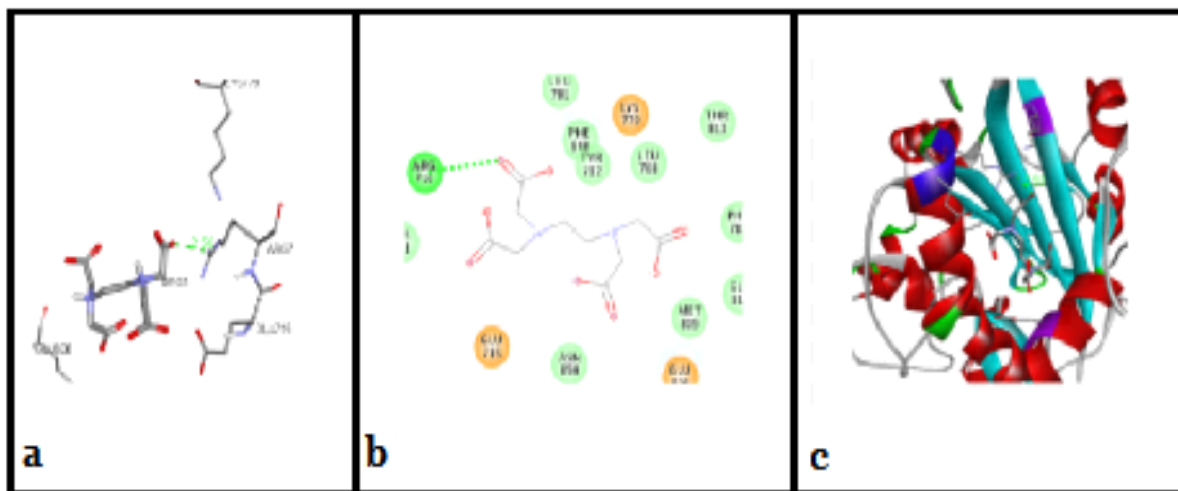


Fig. 12. Figure showing the 3D (a) and 2D (b) ligand interaction of the standard (EDTA) with interacting receptor (PDE) residues and the position of ligand in the binding site of receptor (c).

The docking analysis of CA-II with the ligand (C-1) shows that oxygen of Pro83 form one hydrogen bond with the hydroxyl group of the ligand (Fig.10 (a, b, c)). The bond length was found 2.17Å and the ACE was determined as -93.19 kcal/mol. Three residues of

the receptor CA-II, i.e. Asp85, Pro83 and Thr208 formed three H-bonds with the two methoxy groups and one hydroxyl group of the ligand (C-2), respectively. The ligand binding positions are shown in figure 11 (a, b, c).

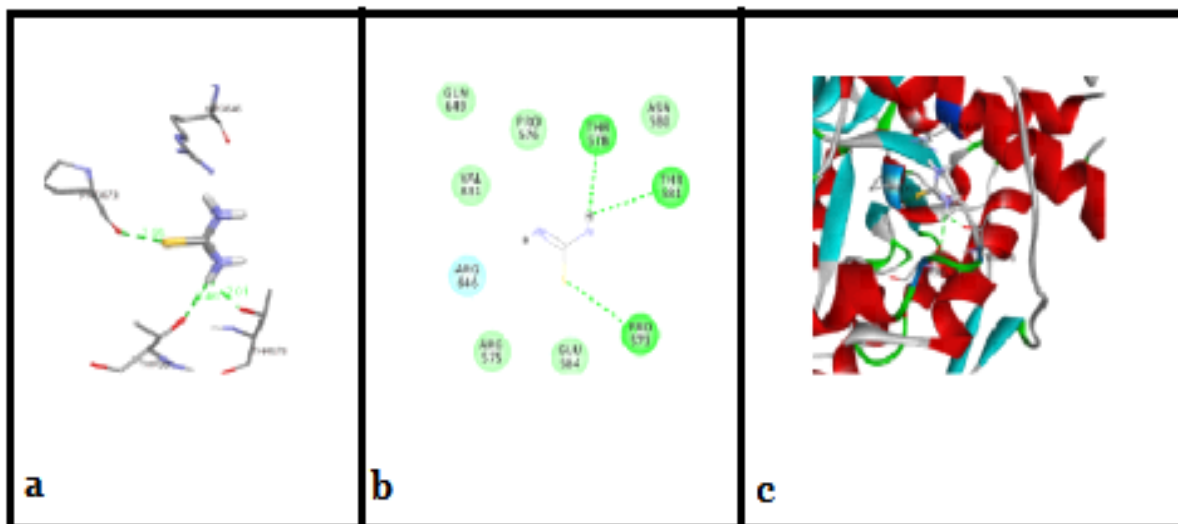


Fig. 13. Figure showing the 3D (a) and 2D (b) ligand interaction of the standard (Thiourea) with interacting receptor (Urease) residues and the position of ligand in the binding site of receptor (c).

The docking analysis of the standard drugs/inhibitors with the corresponding enzymes are shown in figures 12-14. EDTA forms one hydrogen bond with ARG⁷¹⁶ PDE with a bond length 2.50Å who's ACE was

obtained -80.77 kcal/mol. Thiourea form three hydrogen bonds with three residues of urease with ACE -69.61 kcal/mol. Similarly, acetazolamide make one stable interaction with the TYR⁷ of CA-II with

ACE equal to -49.25 kcal/mol. It is clear from the figures that compounds C-1 and C-2 good interactions with the target enzymes as compared to

the standard drugs i.e. EDTA (PDE standard inhibitor), thiourea (Urease standard inhibitor) and Acetazolamide (CA-II standard inhibitor).

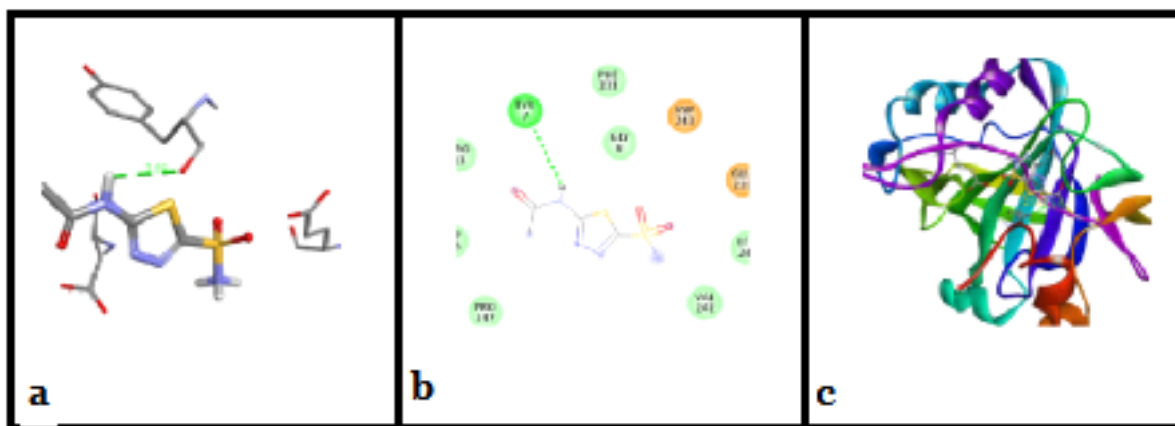


Fig. 14. Figure showing the 3D (a) and 2D (b) ligand interaction of the standard (Acetazolamide) with interacting receptor (CA-II) residues and the position of ligand in the binding site of receptor (c).

References

Arabski M, Konieczna I, Sołowiej D, Rogoń A, Kolesińska B, Kamiński Z, Kaca W. 2010. Are anti-*Helicobacter pylori* urease antibodies involved in atherosclerotic diseases? *Clinical biochemistry* **43(1-2)**, 115-123.

<https://doi.org/10.1016/j.clinbiochem.2009.09.0.16>

Biovia DS, Biovia Workbook Release. 2017. BIOVIA Pipeline Pilot, Release 2017, San Diego: Dassault Systèmes.

Cheminformatics M. 2015. Web-enabled software for large-scale calculation of molecular properties and database searches. Free online molecular descriptor calculations.

Daina A, Michielin O, Zoete V. 2017. SwissADME: a free web tool to evaluate pharmacokinetics, drug-likeness and medicinal chemistry friendliness of small molecules. *Scientific reports* **7**, 42717.

<https://doi.org/10.1038/srep42717>

Deng CM, Liu SX, Huang CH, Pang JY, Lin YC. (2013). Secondary metabolites of a mangrove endophytic fungus *Aspergillus terreus* (No. GX7-3B) from the South China Sea. *Marine drugs* **11(7)**, 2616-

2624.

<https://doi.org/10.3390/md11072616>

Dunn BE, Phadni SH. 1998. Structure, function and localization of *Helicobacter pylori* urease. *The Yale journal of biology and medicine* **71(2)**, 63.

Follmer C. 2010. Ureasases as a target for the treatment of gastric and urinary infections. *Journal of clinical pathology* **63(5)**, 424-430.

Kakiuchi S, Yamazaki R, Teshima Y, Uenishi K, Miyamoto E. 1975. Multiple cyclic nucleotide phosphodiesterase activities from rat tissues and occurrence of a calcium-plus-magnesium-ion-dependent phosphodiesterase and its protein activator. *Biochemical Journal* **146(1)**, 109-120.

<https://doi.org/10.1042/bj14601.09>

Khan AA, Bacha N, Ahmad B, Bakht J, Lutfullah G, Ali J. 2017. Synthesis of secondary metabolites by *Cladosporium resinae* (NRL-6437) under different growth media and chemical inducers and their pharmaceutical activity. *Pakistan journal of pharmaceutical sciences* **30(5)**, 1617-1624.

Khan AA, Bashir A, Lutfullah G, Hussain Z, Bacha N. 2013. Biological Screening of the crude

extract isolated from a soil born fungi *Cladosporium carrionii*. Pakistan Journal of Weed Science Research **19(4)**.

Konieczna I, Kwinkowski M, Kolesinska B, Kaminski Z, Zarnowiec P, Kaca W. 2012. Detection of antibodies against synthetic peptides mimicking ureases fragments in sera of rheumatoid arthritis patients. Protein and peptide letters **19(11)**, 1149-1154.

<https://doi.org/10.2174/092986612803217.123>

Li Q, Csetenyi L, Gadd GM. 2014. Biom mineralization of metal carbonates by *Neurospora crassa*. Environmental science & technology **48(24)**, 14409-14416.

Luo J, Yan Zy, Guo XH, WANG YI. 2007. Isolation, identification and the antibacterial activity of endophytic fungi in *Euphorbia nematocypha* Hand.-Mazz. West China Journal of Pharmaceutical Sciences **22(4)**, 380.

Mills N. 2006. ChemDraw Ultra 10.0 CambridgeSoft, 100 CambridgePark Drive, Cambridge, MA 02140. www.cambridgesoft.com. Commercial Price: 1910fordownload, 2150 for CD-ROM; Academic Price: 710fordownload, 800 for CD-ROM: ACS Publications.

<https://doi.org/10.1021/ja06978.75>

Perry MJ, Higgs GA. 1998. Chemotherapeutic potential of phosphodiesterase inhibitors. Current opinion in chemical biology **2(4)**, 472-481.

[https://doi.org/10.1016/S1367-5931\(98\)801.23-3](https://doi.org/10.1016/S1367-5931(98)801.23-3)

Pretsch A, Nagl M, Schwendinger K, Kreiseder B, Wiederstein M, Pretsch D, Genov M, Hollaus R, Zinssmeister D, Debbab A. 2014. Antimicrobial and anti-inflammatory activities of endophytic fungi *Talaromyces wortmannii* extracts against acne-inducing bacteria. PLOS ONE, **9(6)**, e97929.

Schneidman-Duhovny D, Inbar Y, Nussinov R,

Wolfson HJ. 2005. PatchDock and SymmDock: servers for rigid and symmetric docking. Nucleic acids research **33(2)**, W363-W367.

<https://doi.org/10.1093/nar/gki4.81>

Schüttelkopf AW, Van Aalten DM. 2004. PRODRG: a tool for high-throughput crystallography of protein-ligand complexes. Acta Crystallographica Section D: Biological Crystallography **60(8)**, 1355-1363.

<https://doi.org/10.1107/S0907444904011679>

Şentürk M, Gülçin İ, Beydemir Ş, Küfrevioğlu Öİ, Supuran CT. 2011. In vitro inhibition of human carbonic anhydrase I and II isozymes with natural phenolic compounds. Chemical biology & drug design **77(6)**, 494-499.

Sippl MJ. 1993. Recognition of errors in three-dimensional structures of proteins. *Proteins: Structure, Function, and Bioinformatics* **17(4)**, 355-362.

Strobel G, Ford E, Worapong J, Harper JK, Arif AM, Grant DM, Fung PC, Chau RMW. 2002. Isopestacin, an isobenzofuranone from *Pestalotiopsis microspora*, possessing antifungal and antioxidant activities. Phytochemistry **60(2)**, 179-183.

[https://doi.org/10.1016/S0031-9422\(02\)000.62-6](https://doi.org/10.1016/S0031-9422(02)000.62-6)

Tatum J, Baker R, Berry R. 1985. Naphthoquinones produced by *Fusarium oxysporum* isolated from citrus. Phytochemistry **24(3)**, 457-459.

Vardanyan R, Hruby V. 2016. Synthesis of best-seller drugs: Academic press.

Weber D, Sterner O, Anke T, Gorzalczancy S, Martino V, Acevedo C. 2004. Phomol, a new anti-inflammatory metabolite from an endophyte of the medicinal plant *Erythrina crista-galli*. The Journal of Antibiotics **57(9)**, 559-563.

Wiederstein M, Sippl MJ. 2007. ProSA-web:

interactive web service for the recognition of errors in three-dimensional structures of proteins. *Nucleic acids research* **35(2)**, W407-W410.

<https://doi.org/10.1093/nar/gkm2.90>

Willard L, Ranjan A, Zhang H, Monzavi H, Boyko RF, Sykes BD, Wishart DS. 2003. VADAR: a web server for quantitative evaluation of protein structure quality. *Nucleic acids research*, **31(13)**, 3316-3319.

Xu D, Zhang Y. 2011. Improving the physical realism and structural accuracy of protein models by

a two-step atomic-level energy minimization. *Biophysical journal* **101(10)**, 2525-2534.

<https://doi.org/10.1016/j.bpj.2011.10.0.24>

Zhang Z, Li Y, Lin B, Schroeder M, Huang B. 2011. Identification of cavities on protein surface using multiple computational approaches for drug binding site prediction. *Bioinformatics* **27(15)**, 2083-2088.

<http://dx.doi.org/10.1093/bioinformatics/btr331>